

A surface-anchored molecular four-level conductance switch based on single proton transfer

Willi Auwärter^{†,*}, Knud Seufert[†], Felix Bischoff, David Eciya, Saranyan Vijayaraghavan, Sushobhan Joshi, Florian Klappenberger, Niveditha Samudrala and Johannes V. Barth

The development of a variety of nanoscale applications^{1,2} requires the fabrication and control of atomic^{3–5} or molecular switches^{6,7} that can be reversibly operated by light⁸, a short-range force^{9,10}, electric current^{11,12} or other external stimuli^{13–15}. For such molecules to be used as electronic components, they should be directly coupled to a metallic support and the switching unit should be easily connected to other molecular species without suppressing switching performance. Here, we show that a free-base tetraphenyl-porphyrin molecule, which is anchored to a silver surface, can function as a molecular conductance switch. The saddle-shaped molecule has two hydrogen atoms in its inner cavity that can be flipped between two states with different local conductance levels using the electron current through the tip of a scanning tunnelling microscope. Moreover, by deliberately removing one of the hydrogens, a four-level conductance switch can be created. The resulting device, which could be controllably integrated into the surrounding nanoscale environment, relies on the transfer of a single proton and therefore contains the smallest possible atomistic switching unit.

Porphyrins and related compounds are well established as molecular building blocks in surface-based nanoscale systems due to their inherent functionality, which has been observed in both biological and artificial systems¹⁶. The structural stability of many of these species guarantees a straightforward sublimation in a highly controlled ultrahigh-vacuum environment, and their chemical variability allows the self-assembly of well-defined architectures such as molecular films^{17,18}, porous networks^{19,20}, chains²¹, multideckers²² or metal–molecule contacts²³.

The tetrapyrrole macrocycle can accommodate either a metal ion or two hydrogens. It is well known that the two central protons of a free-base porphyrin readily transfer between the two pairs of opposing nitrogens in the macrocycle (compare Fig. 1d and f) at ambient temperatures, a process called tautomerization^{24,25}. Recently, a pioneering study introduced a bistable conductance switch based on this mechanism, employing naphthalocyanine molecules on thin insulating films¹². The two- and four-level conductance switches described in the following also make use of a tautomerization reaction in individual molecules, but are directly anchored on a metallic support.

To guarantee a stable readout and controlled operation, the molecular switches are studied by scanning tunnelling microscopy (STM) at low temperatures, where the intrinsic proton transfer dynamics is suppressed. STM offers unique opportunities to operate individual switches on the atomic scale^{3–5}. Not only can the local atomic or molecular configurations be probed before and

after flipping the switch, but the operation process itself can be followed by recording, for example, current traces as a function of time²⁶, and can even be modified²⁷.

Figure 1 introduces the free-base tetraphenyl-porphyrin (2H-TPP) molecule, with two hydrogen atoms in the inner cavity. At low temperatures they are localized at opposing nitrogens, resulting in two possible *trans*-type configurations represented by a 90° rotation of the hydrogen pair. High-resolution STM images (Fig. 1a) combined with near-edge X-ray absorption fine structure spectroscopy (NEXAFS) data (Supplementary Fig. S1) demonstrate that on adsorption on the Ag(111) surface, the 2H-TPP molecule adapts to a saddle-shaped macrocycle geometry with pairs of opposite pyrrole rings tilted upwards (α -pyr) or downwards (κ -pyr)^{18,28}, respectively (Fig. 1b). This deformation is linked to rotated terminal phenyl rings by steric repulsion (Fig. 1, Supplementary Fig. S1). Because of the resulting twofold symmetric macrocycle geometry, the two positions of the hydrogen pair are not equivalent. The corresponding two configurations can be stably imaged and directly discriminated in high-resolution STM topographs taken at low bias voltages (Fig. 1c,e). In configuration H_α , the hydrogen pair is aligned with the main axis of the molecule defined by the upward bent α -pyr rings (Fig. 1c,d), while in configuration H_κ , the hydrogen pair is positioned at the κ -pyr units (Fig. 1e,f). Applying a tunnelling current at a voltage exceeding a given threshold can result in a reversible switching between configurations H_α and H_κ that we attribute to an induced transfer of the proton pair. Other origins cannot explain the observed transformations: a conformational switching of the macrocycle would induce a rotation of the terminal phenyl legs. However, high-resolution STM data, characterizing the orientation of the phenyl groups, show no difference related to the legs upon switching. Thus, a macrocycle adaptation is ruled out. In addition, deprotonation experiments clearly indicate that the positions of the inner hydrogens determine the two configurations H_α and H_κ . At low bias voltages, both configurations can be imaged stably, guaranteeing a reliable readout of the switch. Throughout this Letter, use of the wording hydrogen atom or pair describes static configurations, whereas dynamic processes are termed proton transfer.

The double proton transfer induced by applying a tunnelling current can be monitored directly by recording the tunnelling current I versus time t . To this end, the tip is positioned over one of the α -pyr rings (Fig. 1c), the tunnelling parameters (I , U) are set and the feedback loop is opened. The proton transfer can be triggered at any position above the molecule; however, the rate is generally lower on the κ -pyr rings due to the twofold macrocycle symmetry (Fig. 1g, Supplementary Fig. S2) and drops to zero on the

Physik Department E20, Technische Universität München, D-85748 Garching, Germany; [†]These authors contributed equally to this work.

*e-mail: wau@tum.de

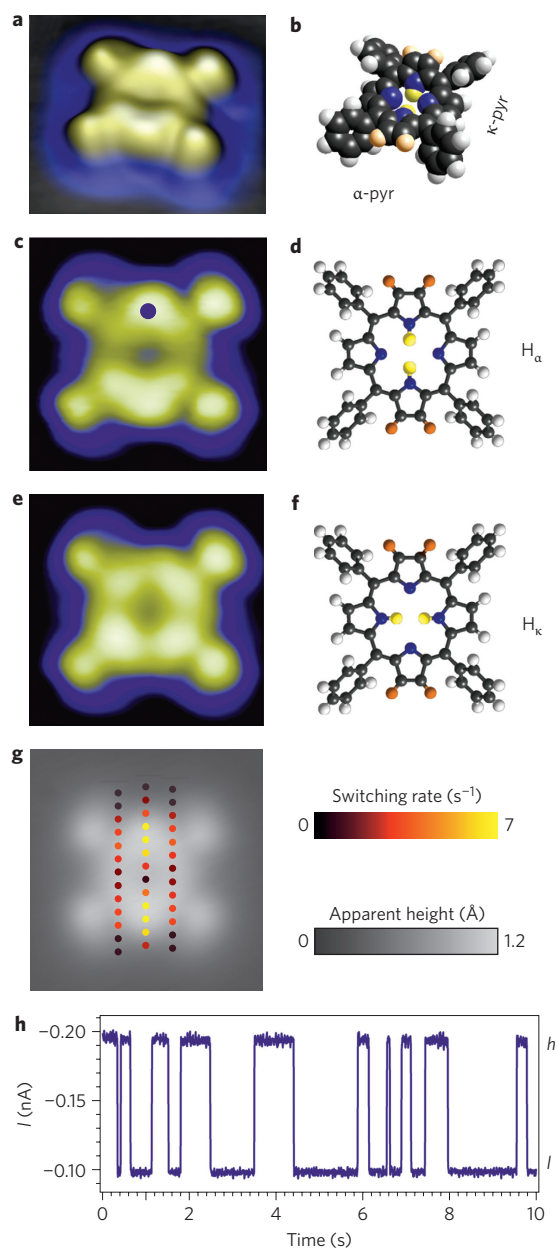


Figure 1 | Double proton transfer in 2H-TPP on Ag(111). **a**, Pseudo three-dimensional rendering of a high-resolution STM image of 2H-TPP adsorbed on Ag(111). **b**, Corresponding model consistent with the NEXAFS data (cf. Supplementary Fig. S1) highlights the saddle-shaped deformation resulting in two inequivalent pairs of pyrrole rings (α -pyr, marked in orange, and κ -pyr). **c**, STM image of configuration H_α ($I = 0.1$ nA, $U = -0.2$ V). **d**, Model highlighting the saddle-shaped deformation and the position of the hydrogen pair in configuration H_α . **e**, STM image of configuration H_κ ($I = 0.1$ nA, $U = -0.2$ V). **f**, Model of configuration H_κ . **g**, Spatial dependence of the switching rate displayed with colour-coded dots (recorded at -1.6 V and 2 nA). The highest rates (yellow markers) are observed above the α -pyr. **h**, Current versus time trace recorded at -1.9 V at the position indicated in **c**. A switching between two current levels representing the high (h) and low (l) conductance states is clearly discernible.

bare metal next to the molecule. A typical $I(t)$ trace is presented in Fig. 1h and clearly reveals a switching between two well-defined current levels. The high conductance state h represents configuration H_α and the low conductance state l corresponds to configuration H_κ , as inferred from a comparison with the apparent

heights of both pyrrole moieties in the STM images. Thus, 2H-TPP/Ag(111) represents a bistable system. A detailed discussion of the switching rate and the underlying mechanism follows; however, it needs to be emphasized that we detected, at most, two current levels in all data on 2H-TPP, covering switching rates up to 0.5 kHz. Even after ordering 2H-TPP molecules in highly regular square arrays on Ag(111), the switching operation is demonstrated (Supplementary Fig. S3).

To upgrade this bistable system to a four-level conductance switch, we applied an atomically controlled deprotonation procedure in which the STM tip was centred above the 2H-TPP macrocycle and a voltage pulse of typically 2 V was applied, resulting in the removal of one of the inner protons. This single deprotonation process, yielding a 1H-TPP species, can be directly monitored in $I(t)$ traces (shown in Fig. 2g). Furthermore, a complete deprotonation of the macrocycle pocket can be achieved by a second step²⁹ using a voltage pulse of typically 2.2 V. STM images representing all three species, that is, 2H-TPP, 1H-TPP and 0H-TPP, are shown in Fig. 2a–c together with corresponding schematic models (Fig. 2d–f). All these deprotonation events are irreversible. The deprotonated 0H-TPP is of no further interest, as complete macrocycle deprotonation prevents any proton-related switching events, as confirmed experimentally. In contrast, the singly deprotonated 1H-TPP offers the possibility that the remaining hydrogen can be localized at each of the four nitrogen positions in the porphyrin pocket.

Figure 3 presents all four configurations for the 1H-TPP molecule: $H_{\alpha 1}$, $H_{\kappa 1}$, $H_{\kappa 2}$ and $H_{\alpha 2}$. As in the 2H-TPP case, low-voltage imaging allows us to read out the position of the hydrogen, while higher voltages induce switching, which can be tracked by means of $I(t)$ spectra. The trace in Fig. 2g indicates that a switching can be observed even after the first deprotonation. On positioning the STM tip in a slightly asymmetric position above a pyrrole ring, up to four different current levels can be discriminated (Fig. 3i, Supplementary Fig. S5). In analogy to the 2H-TPP case, we relate these four conductance states to the position of the hydrogen in the porphyrin pocket (Fig. 3e–h). We observe the highest conductance if the hydrogen is located at the κ -pyr where the tip is positioned. The two subjacent levels represent the positions on the two neighbouring α -pyr rings and the lowest conduction level represents the opposing κ -pyr location, respectively, as confirmed experimentally. It should be noted that a suitable positioning of the tip is crucial to detect all four current levels. In the case where a sharp tip would be perfectly centred above the macrocycle, only two current levels, representing the inequivalent pyrroles α -pyr and κ -pyr, could be distinguished due to symmetry reasons.

The limited time resolution in the spectrum in Fig. 3i implies that the proton can not only be exchanged between neighbouring nitrogens, but can also be directly transferred to the opposing nitrogen, as indicated for example by the transition from the highest to the lowest conductance level observed at a time of 2.2 s. However, a careful analysis reveals that the transitions typically proceed through the intermediate levels. These experiments clearly indicate that the hydrogen position can be directly identified in constant-current STM images. Also, a readout of a given current value unambiguously determines the configuration. However, it should be noticed that the observed protrusions do not represent the hydrogen itself, but rather the electronic effect reflecting its presence at the pyrrole rings of the porphyrin macrocycle. Applying a single switching event, the proton cannot be deliberately transferred to one specific position. However, this does not hamper the function of the switch, as the current levels that are recorded during operation of the switch are characteristic for the proton position and a feedback mechanism might be used to freeze the desired state. In addition, there is some control over the switching direction. The residence time in the highest current state is shortest, as clearly seen, for example, in Supplementary Fig. S5b. Thus we

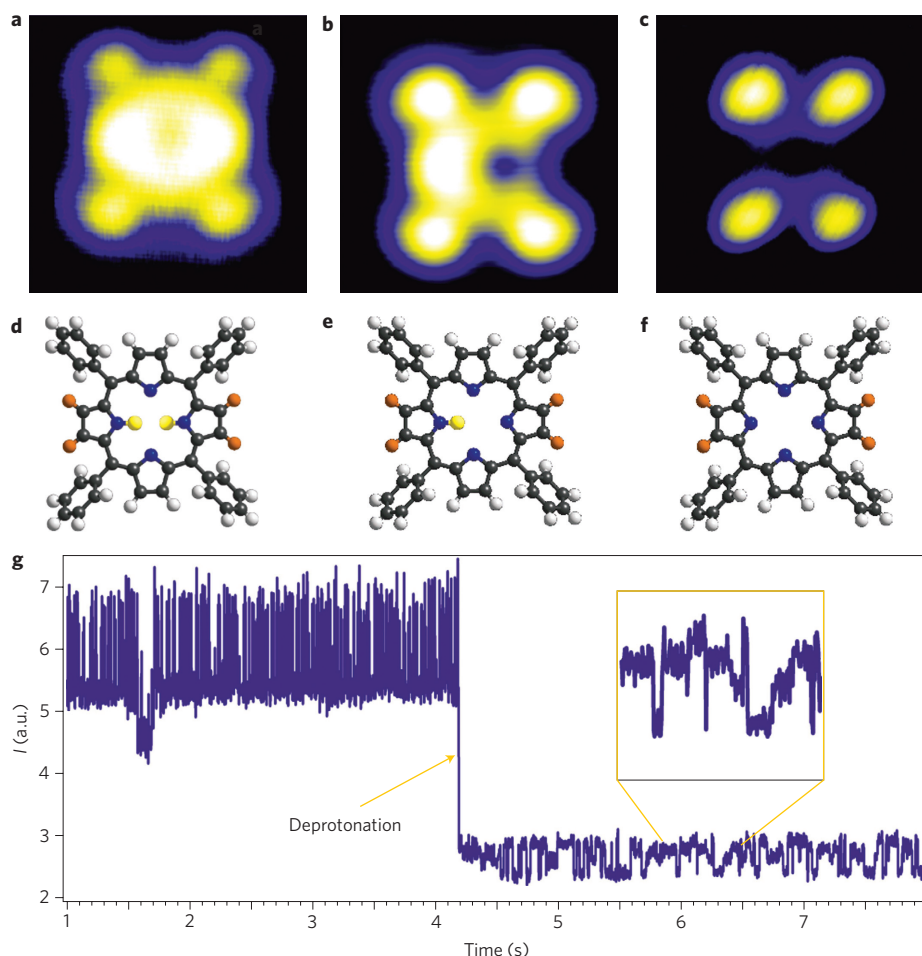


Figure 2 | Sequential deprotonation of 2H-TTP on Ag(111). **a**, STM image of 2H-TTP ($I = 0.2$ nA, $U = -0.2$ V). **b**, STM image of 1H-TTP. **c**, STM image of OH-TTP. **d–f**, Tentative models illustrating the 2H-TTP, singly deprotonated 1H-TTP and fully deprotonated OH-TTP species. **g**, $I(t)$ trace recorded at the centre of 2H-TTP at 1.9 V. The sudden decrease in current represents the single deprotonation to 1H-TTP.

deal with a configuration where the proton residence time on the pyrrole close to the tip position is lower than on the other positions.

To clarify the proton transfer mechanism, tens of thousands of switching events at different sample bias voltages U and tunnelling currents I were evaluated for both the 2H-TTP and 1H-TTP cases. The analysis is summarized in Fig. 4 (current dependence) and Fig. 5 (voltage dependence). These plots rely on data recorded with the STM tip close to an α -pyr position.

The linear current dependence of switching rate S (Fig. 4) points to a one-electron process driving the proton transfer in 2H-TTP and 1H-TTP. This finding is corroborated by an analysis of the switching times presented in Supplementary Fig. S4. In combination with the voltage-dependent data presented below, we thus exclude the electric field between tip and molecule as the dominating trigger for the tautomerization process. Nevertheless, as shown in Supplementary Fig. S6, the absolute switching rate depends on the termination of the STM tip and thus on the current density. A direct comparison of the switching rates between 2H-TTP and 1H-TTP was therefore performed with the same tip on the very same molecule before and after deprotonation. The linear fits in Fig. 4b reveal that the switching rates for 1H-TTP ($S_{1\text{H-TTP}}$; see Supplementary Information for a discussion of the data analysis, Supplementary Fig. S7) and 2H-TTP ($S_{2\text{H-TTP}}$) are similar. However, the ratio $S_{1\text{H-TTP}}/S_{2\text{H-TTP}} = 1 \pm 0.4$ varies from molecule to molecule. This scatter might originate in minute modifications of the tip or subtle differences in the adsorption configuration

during the deprotonation procedure and is beyond control in our experiments. However, importantly, the rate for 1H-TTP corresponds approximately to the rate for 2H-TTP at any given current value. Accordingly, in both cases a similar number of electrons are needed for one switching event, which points to an analogous process for switching in both species.

Regarding the voltage dependence summarized in Fig. 5, for bias voltages below ± 0.5 V no switching events could be detected, confirming the stable readout by STM images at low bias. Above this threshold, the switching rate S increases by several orders of magnitude within 1 V for both 2H-TTP and 1H-TTP. In a small voltage range between ± 1 and ± 1.5 V the increase is nearly exponential and levels off at higher voltages¹². Figure 5a includes voltage-dependent data recorded at three constant current values (0.5, 2 and 4 nA, normalized to a rate of 1 at -1.5 V) that show identical behaviour. The very similar rates for positive and negative sample bias voltages, resulting in curves symmetric to the Fermi level (Fig. 5a), exclude an exclusive role of one specific molecular orbital in the proton transfer. Indeed, tunnelling spectra recorded above an α -pyr show a highly asymmetric local electronic density of states around the Fermi level (Fig. 5b). This is of importance, as recent theoretical models addressing surface-anchored switches based on tautomerization solely consider an electron transfer via the lowest unoccupied molecular orbital (LUMO)^{30,31}. The fact of the voltage threshold and symmetry agreeing for both polarities rather points to an excitation of the proton transfer by electrons

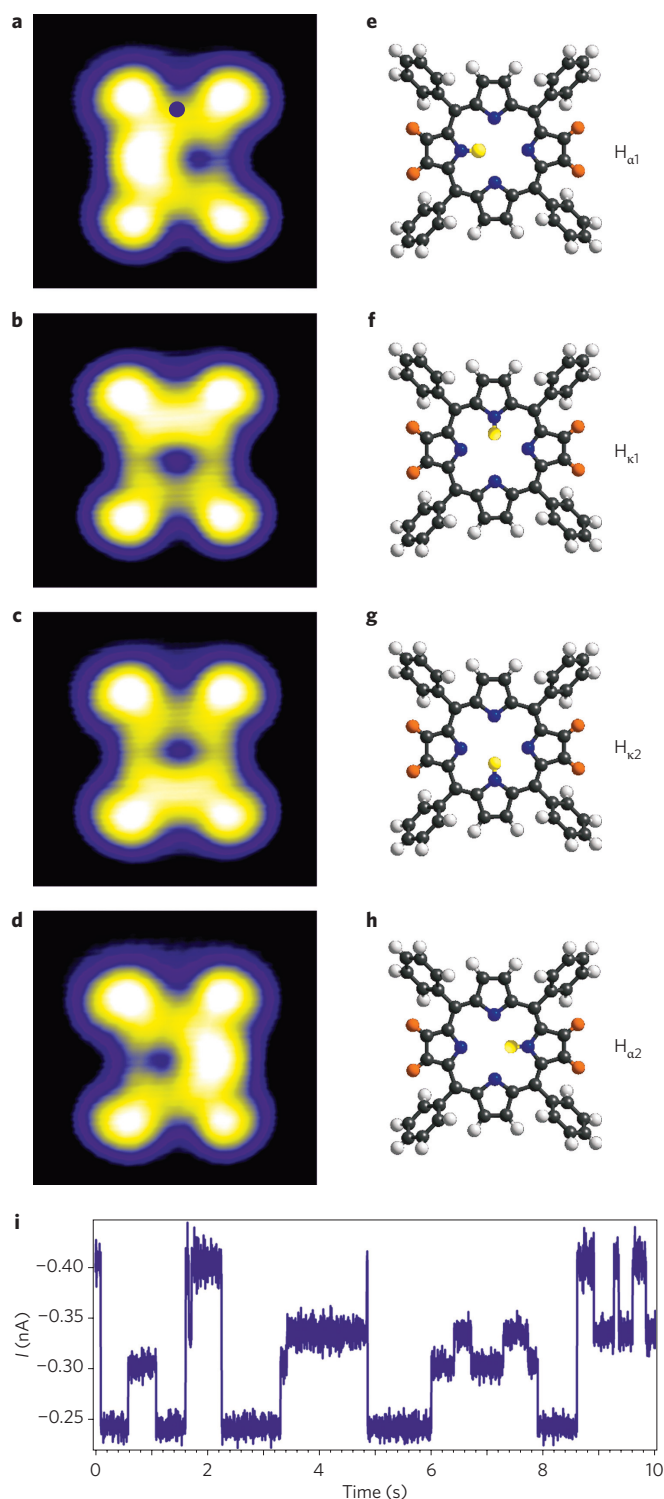


Figure 3 | Visualization of the four proton positions in 1H-TPP on Ag(111). **a–h**, STM images (**a–d**) of the same 1H-TPP molecule in four configurations representing the hydrogen positions schematically shown in corresponding models **e–h** ($I = 0.2$ nA, $U = -0.2$ V). **i**, Current trace recorded in a slightly asymmetric position on a κ -pyr position (marked by the dot in **a**). The four conductance levels are clearly discernible ($I = 0.4$ nA, $U = -1.6$ V).

tunnelling inelastically through the porphyrin. Indeed, it is generally agreed that the proton transfer in free-base porphyrins involves both vibrational excitations in the macrocycle that temporarily reduce the separation of the hydrogen from an adjacent nitrogen

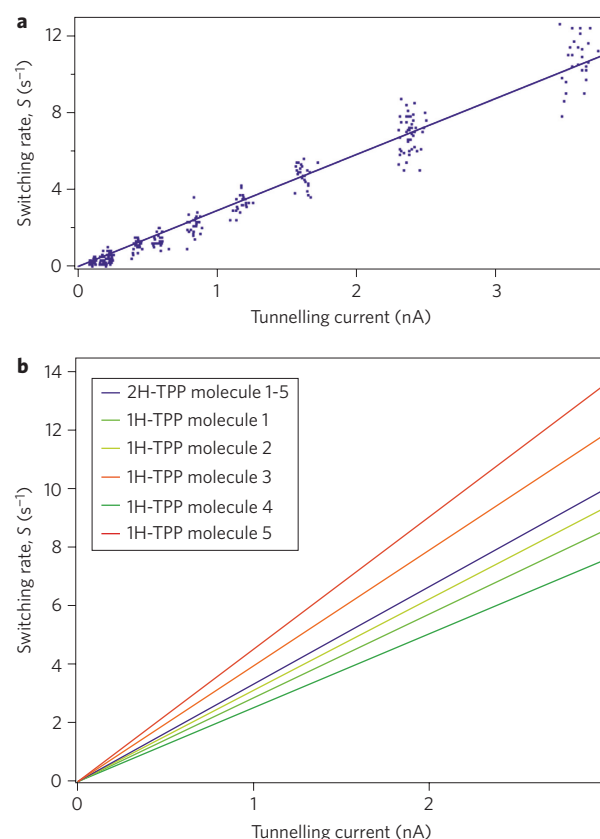


Figure 4 | Current dependence of switching rate S for 2H-TPP and 1H-TPP recorded on an α -pyr position. **a**, S increases linearly with tunnelling current I , pointing to a one-electron process driving proton transfer. Every single data point represents one $I(t)$ spectrum where the current is averaged over the whole spectrum. The absolute rate depends on tip geometry (see Supplementary Information). The tip used for this experiment yields a rate S_{2H-TPP} of 3.0 ± 0.1 s $^{-1}$ nA $^{-1}$ at a constant voltage of -1.6 V. **b**, Comparison of S for 2H-TPP and 1H-TPP for five molecules. The blue line represents the normalized fits for the 2H-TPP species. Normalization to one average rate for 2H-TPP was performed to ease the comparison to 1H-TPP as the absolute rates for 2H-TPP vary from molecule to molecule. The green and red lines show the corresponding rates for the same molecules measured with an identical tip after the first deprotonation. Although the rates are generally similar for 2H-TPP and 1H-TPP, the ratio S_{1H-TPP}/S_{2H-TPP} varies between 0.76 (dark green) and 1.36 (dark red).

site, and proton tunnelling. The corresponding barrier heights, determined by theoretical and experimental studies, range from 0.5 to 0.6 eV (refs 29,31–33) and thus coincide with the onset voltage observed in our experiments. Overall, the peculiar voltage dependence of the switching rate calls for thorough theoretical studies.

Adjusting I and U , S can be tuned easily from 0 to ~ 500 Hz, reaching quantum yields (events per electron) of $\sim 7 \times 10^{-7}$ (Supplementary Fig. S8). The limitations in switching frequency are given by both the voltage threshold for deprotonation and lateral displacements of the molecule induced at high currents.

The obvious similarity between 2H-TPP and 1H-TPP in both the current and voltage dependence suggests that the same process is involved in the switching. This is in full agreement with most current studies, which agree that the double proton migration in liquid and solid states proceeds in a stepwise, asynchronous manner involving an intermediate state^{32,34,35}. The scheme in Fig. 5c sketches this reaction pathway. Instead of an immediate,

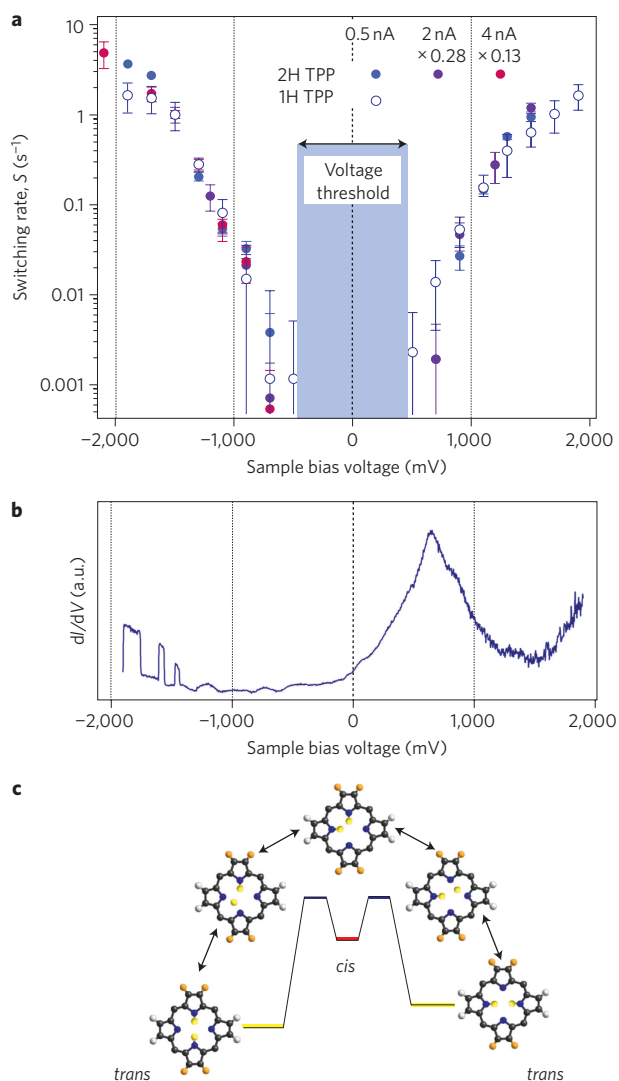


Figure 5 | Voltage dependence of the switching rate S for 2H-TPP and 1H-TPP excited on an α -pyr position. **a**, Voltage dependences measured at constant currents of 0.5, 2 and 4 nA, respectively, showing a threshold for switching of ~ 500 mV followed by a sharp increase with similar slope for both polarities (all data points were normalized to 1 at -1.5 V using scaling factors of 0.28 and 0.13, respectively). **b**, Characteristic scanning tunnelling spectra recorded above an α -pyr position of 2H-TPP representing the local density of states, which is clearly asymmetric for both polarities. The broad feature around 700 mV is identified as the LUMO, whereas no occupied resonance is observed at negative bias voltages. The discontinuities observed at elevated voltages of both polarities are effects of proton transfer. **c**, Scheme sketching the stepwise proton transfer via a *cis*-like intermediate state for 2H-TPP (the phenyl groups are omitted for clarity; see text for discussion). The macrocycle deformation on adsorption potentially lifts the degeneracy of both *trans*-configurations.

synchronous migration of both protons, they are transferred one by one. The intermediate state is characterized by a *cis*-type configuration where the two hydrogens occupy neighbouring nitrogen sites. Judging from the literature, the *cis*-state has a very short lifetime^{32,35} and relaxes either back to the initial state or to the final rotated configuration (Fig. 5c). Hence, the *cis*-state decays immediately on the timescale of a typical STM experiment and is not detectable. Accordingly, from a practical point of view, the 2H-TPP/Ag(111) indeed constitutes a two-level conductance switch and recent theoretical suggestions claiming four conductance

levels detectable by STM in a related system seem rather optimistic³¹. Assuming that the switching process is triggered by a direct excitation of hydrogens by tunnelling electrons, the observed similarities between 2H-TPP and 1H-TPP indicate that in both cases one proton is transferred to an adjacent nitrogen site for each excitation. This interpretation substantiates the idea that for a metal surface-anchored porphyrin too, the tautomerization reaction proceeds in an asynchronous way. If, on the other hand, the switching originates in a deformation of the macrocycle induced by tunnelling electrons and the resulting proton transfer is not the rate-limiting process, an immediate or asynchronous motion cannot be discriminated.

In summary, we have developed a novel metal-anchored four-level conductance switch based on prototropy. Specifically, an individual proton is reversibly transferred in the macrocycle of a singly deprotonated 1H-TPP molecule. Thus, we have provided a demonstration of the smallest possible atomistic switching unit. The direct comparison to 2H-TPP/Ag(111) (representing a bistable system with two well-defined conductance levels) allows us to gain insight into the proton transfer mechanism on which the switches are based. The data point to a one-electron-induced excitation as a trigger for proton migration in both species and suggest an identical switching process in both 1H-TPP and 2H-TPP. As the periphery of the molecule is not affected by the proton migration in the inner pocket, the switch is integrable into nanoscale architectures. During the operation of the switch, the STM tip is stationary and only plays the role of the second electrode. Consequently, just an appropriate electrode, and no complete STM set-up, is needed for the switching action. All the above features reveal the promise of the free-base TPP species presented here for future nanoscale applications, especially as our findings might be easily extended to the huge class of other free-base porphyrins as well as related macrocyclic compounds.

Methods

All experiments were performed in a custom-designed ultrahigh-vacuum chamber housing a commercial STM operated at 6 K (www.lt-stm.com). The base pressure during the experiments was below 2×10^{-10} mbar. Repeated cycles of Ar^+ sputtering and annealing to 725 K were used to prepare the Ag(111) single crystal. Subsequently, 2H-TPP molecules (Sigma Aldrich, purity $\geq 99\%$) were dosed from a thoroughly degassed quartz crucible held at 600 K. During deposition the sample temperature was kept at room temperature to grow 2H-TPP arrays or at 150 K to obtain individual 2H-TPP molecules. All STM images were recorded in constant-current mode using an electrochemically etched tungsten tip prepared by sputtering and controlled dipping into the Ag(111) substrate. In the figure captions U refers to the bias voltage applied to the sample. The WsXM program (www.nanotec.es) was used to display the STM images. Current traces $I(t)$ were recorded at constant height (open feedback loop) after setting the desired parameters (I , U).

Received 13 June 2011; accepted 31 October 2011;
published online 11 December 2011

References

- Browne, W. R. & Feringa, B. L. Making molecular machines work. *Nature Nanotech.* **1**, 25–35 (2006).
- Balzani, V., Credi, A. & Venturi, M. Molecular machines working on surfaces. *ChemPhysChem* **9**, 202–220 (2008).
- Eigler, D. M., Lutz, C. P. & Rudge, W. E. An atomic switch realized with the scanning tunnelling microscope. *Nature* **352**, 600–603 (1991).
- Repp, J., Meyer, G., Olsson, F. E. & Persson, M. Controlling the charge state of individual gold adatoms. *Science* **305**, 493–495 (2004).
- Quaade, U. J., Stokbro, K., Thirstrup, C. & Grey, F. Mechanism of single atom switch on silicon. *Surf. Sci.* **415**, L1037–L1045 (1998).
- Donhauser, Z. J. *et al.* Conductance switching in single molecules through conformational changes. *Science* **292**, 2303–2307 (2001).
- Iancu, V. & Hla, S.-W. Realization of a four-step molecular switch in scanning tunneling microscope manipulation of single chlorophyll- α molecules. *Proc. Natl Acad. Sci. USA* **103**, 13718–13721 (2006).
- Wolf, M. & Tegeder, P. Reversible molecular switching at a metal surface: a case study of tetra-tert-butyl-azobenzene on Au(111). *Surf. Sci.* **603**, 1506–1517 (2009).

9. Loppacher, C. *et al.* Direct determination of the energy required to operate a single molecule switch. *Phys. Rev. Lett.* **90**, 066107 (2003).
10. Moresco, F. *et al.* Conformational changes of single molecules induced by scanning tunneling microscopy manipulation: a route to molecular switching. *Phys. Rev. Lett.* **86**, 672–675 (2001).
11. Henzl, J., Mehlhorn, M., Gawronski, H., Rieder, K.-H. & Morgenstern, K. Reversible *cis-trans* isomerization of a single azobenzene molecule. *Angew. Chem. Int. Ed.* **45**, 603–606 (2006).
12. Liljeroth, L., Repp, J. & Meyer, G. Current-induced hydrogen tautomerization and conductance switching of naphthalocyanine molecules. *Science* **317**, 1203–1206 (2007).
13. Pivetta, M., Ternes, M., Patthey, F. & Schneider, W.-D. Diatomic molecular switches to enable the observation of very-low-energy vibrations. *Phys. Rev. Lett.* **99**, 126104 (2007).
14. Wäckerlin, C. *et al.* Controlling spins in adsorbed molecules by a chemical switch. *Nat. Commun.* **1**, 61 (2010).
15. Qiu, X. H., Nazin, G. V. & Ho, W. Mechanisms of reversible conformational transition in a single molecule. *Phys. Rev. Lett.* **93**, 196806 (2004).
16. Dolphin, D. (ed.) *The Porphyrins* (Academic, 1978).
17. Scudiero, L., Barlow, D. E. & Hipps, K. W. Physical properties and metal ion specific scanning tunneling microscopy images of metal(II) tetraphenylporphyrins deposited from vapor onto gold(111). *J. Phys. Chem. B* **104**, 11899–11905 (2000).
18. Auwärter, W. *et al.* Site-specific electronic and geometric interface structure of Co-tetraphenyl-porphyrin layers on Ag(111). *Phys. Rev. B* **81**, 245403 (2010).
19. Spillmann, H. *et al.* A two-dimensional porphyrin-based porous network featuring communicating cavities for the templated complexation of fullerenes. *Adv. Mater.* **18**, 275–279 (2006).
20. Ćija, D. *et al.* Hierarchic self-assembly of nanoporous chiral networks with conformationally flexible porphyrins. *ACS Nano* **4**, 4936–4942 (2010).
21. Heim, D. *et al.* Self-assembly of flexible one-dimensional coordination polymers on metal surfaces. *J. Am. Chem. Soc.* **132**, 6783–6790 (2010).
22. Ćija, D. *et al.* Assembly and manipulation of rotatable cerium porphyrinato sandwich complexes on a surface. *Angew. Chem. Int. Ed.* **50**, 3872–3877 (2011).
23. Nazin, G. V., Qiu, X. H. & Ho, W. Visualization and spectroscopy of a metal-molecule-metal bridge. *Science* **302**, 77–81 (2003).
24. Hennig, J. & Limbach, H.-H. Kinetic study of hydrogen tunnelling in meso-tetraphenylporphyrin by nuclear magnetic resonance lineshape analysis and selective T1ρ-relaxation time measurements. *J. Chem. Soc. Faraday Trans. 2* **75**, 752–766 (1979).
25. Butenhoff, T. J. & Moore, C. B. Hydrogen atom tunneling in the thermal tautomerism of porphine imbedded in a *n*-hexane matrix. *J. Am. Chem. Soc.* **110**, 8336–8341 (1988).
26. Lastapis, M. *et al.* Picometer-scale electronic control of molecular dynamics inside a single molecule. *Science* **308**, 1000–1003 (2005).
27. Martin, M. *et al.* Mastering the molecular dynamics of a bistable molecule by single atom manipulation. *Phys. Rev. Lett.* **97**, 216103 (2006).
28. Seufert, K. *et al.* *Cis*-dicarbonyl binding at cobalt and iron porphyrins with saddle-shape conformation. *Nature Chem.* **3**, 114–119 (2011).
29. Sperl, A., Kröger, J. & Berndt, R. Controlled metalation of a single adsorbed phthalocyanine. *Angew. Chem. Int. Ed.* **50**, 5294–5297 (2011).
30. Sarhan, A., Arboleda, N. B. Jr, David, M., Nakanishi, H. & Kasai, H. STM-induced switching of the hydrogen molecule in naphthalocyanine. *J. Phys. Condens. Matter* **21**, 064201 (2009).
31. Fu, Q., Yang, J. & Luo, Y. Mechanism for tautomerization induced conductance switching of naphthalocyanine molecule. *Appl. Phys. Lett.* **95**, 182103 (2009).
32. Baker, J., Kozłowski, P. M., Jarzecki, A. A. & Pulay, P. The inner-hydrogen migration in free base porphyrin. *Theor. Chem. Acc.* **97**, 59–66 (1997).
33. Braun, J., Hasenfratz, C., Schwesinger, R. & Limbach, H.-H. Free acid porphyrin and its conjugated monoanion. *Angew. Chem. Int. Ed.* **33**, 2215–2217 (1994).
34. Ghosh, A. First-principles quantum chemical studies of porphyrins. *Acc. Chem. Res.* **31**, 189–196 (1998).
35. Maity, D. K., Bell, R. L. & Truong, T. N. Mechanism and quantum mechanical tunneling effect on inner hydrogen atom transfer in free base porphyrin: a direct *ab initio* dynamics study. *J. Am. Chem. Soc.* **122**, 897–906 (2000).

Acknowledgements

The authors thank J. Repp for helpful suggestions concerning the data analysis. The work was supported by the ERC Advanced Grant MolArt (no. 247299), TUM-IAS and the Munich Center for Advanced Photonics (MAP). N.S. acknowledges a scholarship from DAAD. D.E. thanks the European Commission for support through the Marie Curie IntraEuropean Fellowship for Career Development FP7 programme.

Author contributions

K.S., W.A., F.B., D.E., S.V., S.J. and N.S. performed the STM experiments and analysed and interpreted the experimental data. F.K. supported the data analysis and contributed to the NEXAFS experiments. W.A., K.S. and J.V.B. conceived the studies and co-wrote the paper.

Additional information

The authors declare no competing financial interests. Supplementary information accompanies this paper at www.nature.com/naturenanotechnology. Reprints and permission information is available online at <http://www.nature.com/reprints>. Correspondence and requests for materials should be addressed to W.A.